ADVANCED FUNCTIONAL MATERIALS
www.afm-journal.de

Fractal Inorganic–Organic Interfaces in Hybrid Membranes for Efficient Proton Transport

Vasana Maneeratana, John D. Bass, Thierry Azaïs, Amaury Patissier, Karine Vallé, Manuel Maréchal, Gérard Gebel, Christel Laberty-Robert, and Clément Sanchez*

A facile method for preparing highly conductive hybrid organic–inorganic membranes is reported. These membranes are synthesized using an electrospinning process with a sol–gel-based solution containing PVDF–HFP (polyvinylidenefluoride-hexafluoropropylene), functionalized or not functionalized silicon alkoxides, and additives. Proton conduction measurements highlight that these hybrid membranes exhibit conductivity value of 101 mS/cm at 120 °C under 80% RH (relative humidity), comparable to the best Nafion measured under the same conditions. These membranes have a proton conductivity-humidity variation close to Nafion and a modulus value higher than that for Nafion above 80 °C. Their proton conductivity value is about 15 mS/cm under 50% RH, and it constitutes one of the highest values reported. These interesting properties are related to the microstructure of the electrospun membranes that have been characterized using field emission scanning electron microscopy (FE-SEM) and small angle neutron scattering (SANS). The electrospun membranes are made composed of a bundle of fibers surrounded by a functionalized silica network. The bundle of fibers corresponds to the assembly of small polymer fibers surrounded by small anisotropic functionalized silica domains. Coupling the reactive chemistry of the sol–gel-based process with electrospinning allows the design of hybrid membranes with fractal hydrophobic/hydrophilic interfaces exhibiting different length scales.

1. Introduction

Progress in fuel cell technologies relies on replacement of Nafion by hybrid organic-inorganic membranes.[1–5] The mechanical properties, the swelling and the conduction in these membranes can be tune through the control of the microstructure by using of at least two components. Hybrid organic-inorganic membranes are often defined by discrete, intermingled hydrophilic and hydrophobic domains. Different concepts for hybrid organic-inorganic membranes have been developed.[1–5] Currently, we are interested in the design of hybrid membranes for which conduction properties and robustness, mechanical properties have been separated into two main components. The inorganic moieties support the proton conduction while the organic ones guarantee the mechanical and chemical robustness of the system. Accordingly, the idea is to reproduce the Nafion behavior, wherein a phase separation between hydrophilic and hydrophobic components exists at different scale from a few nanometers up to several micrometers.[6–11] This phase separation contributes to its ion conduction performance. Controlling our processing with sol-gel chemistry in mind, this phase segregation can be tuned with ranges from the nano- to the macroscale, giving rise to membranes with different bulk properties such as proton and water transport.[2–5] The inherent structural characteristics of these hybrid organic-inorganic membranes are highly beneficial for proton exchange membrane fuel cell (PEMFC) working at a high temperature (≈120 °C, 50% relative humidity (RH)), where the inorganic materials facilitates the transport of proton and the water management, and the organic materials brings softness, tightness, processability to the overall systems.

In the literature, different approaches have been explored to design hybrid membrane based on non-conductive or conductive fluorinated polymer.[1,2] The in situ growth of the functionalized or not inorganic network into a conductive fluorinated polymer conduce to a slight improvement of the conductivity value with the humidity content. Pre-formed functionalized inorganic particles with different diameter dispersed into a

Dr. V. Maneeratana, Dr. J. D. Bass, Dr. T. Azaïs, A. Patissier, Prof. C. Laberty-Robert, Prof. C. Sanchez
UPMC Univ Paris 06–Collège de France–CNRS
UMR 7574, Chimie de la Matière Condensée de Paris
Collège de France, 75231 Paris Cedex 05, France
E-mail: christel.laberty@upmc.fr
Dr. K. Vallé
CEA, DAM, Le Ripault, 37260 Monts, France
Dr. M. Maréchal
CNRS-Université de Grenoble,
UMR 5279, Laboratoire d'Electrochimie & de Physico-chimie des Matériaux & des Interfaces
38402 Saint Martin d'Hères, France
Dr. G. Gebel
UJF-CNRS-CEA
UMR 5819, Structure & Propriétés d'Architectures Moléculaires
CEA Grenoble, INAC, 38054 Grenoble 9, France

DOI:10. 1002/adfm.201202701

non conductive polymer give rise to membranes with proton conductivity values comparable to Nafion. But, unfortunately the modification of the dimension of the membrane with the humidity content is important, limiting their use in a real PEMFC.[6] It is only recently that hybrid organic-inorganic materials (organic material:non-conductive polymer) have been both synthesized in proton conductive, PEMFC-relevant compositions and then characterized at its working temperature, e.g., 120 °C, 50%RH.[12]

An earlier sol-gel route was based on growing in-situ functionalized silica networks in a non-conductive thermostable polymer, PVDF-HFP. A modification of the organic-inorganic interface by using a designed terpolymer containing $-SO_3H$ and silane groups allowed an improvement of the proton transport of these hybrid membranes.[3] Conductivity values of 42 mS/cm at 60 °C under 80 RH% were reported; this value is quite high taking into account that the Ion Exchange Capacity (IEC) value is only 0.4 meq/g. This is different from what it has been observed on perfluorosulfonic membranes (PFSA), where the conductivity value is proportional to the IEC values. A decrease in the IEC values from 0.9 to 0.4 meq/g conduces to a decrease in the conductivity value by a factor 4.[8] However, investigation throughout a range of processing conditions (humidity, volume of evaporated solution) and variety of sol-gel conditions (different silica content, different type of ORMOSILs, additives) showed that only a very narrow range of synthesis conditions led to such hybrid membranes with conductivity values in the range of 15 mS/cm at ambient temperature. More than the IEC value, the shape, the connectivity of the inorganic network into the non-conductive polymer matrix influences the proton transport. Oftentimes, the respective proton transport was very much dependent on the humidity conditions; conductivity values of 1 mS/cm at 60 °C for RH = 80% has been measured for several membranes with various compositions.[2,4] In general, hybrid organic-inorganic membranes have been reported with subsequent attempts involving the casting approach to produce membranes leading to poor performance. This suggests that the sol-gel approach combined with spray drying and casting protocols conduces to the formation of membranes with a non through-connected silica network or/and that the surface of the membrane is highly hydrophobic, limiting insertion of proton in the membrane.[13] Nonetheless, these trends result most often in non continuous proton pathways throughout the non-conductive polymeric matrix.

2. Results and Discussion

Our approach to synthesize these current hybrid membranes is based on the electrospinning process coupled with the sol-gel chemistry (**Figure 1**a).[14] This protocol, combining hybrid organic-inorganic solutions and electrospinning, is a novel approach for preparing hybrid membranes with 3D continuous interconnected inorganic proton pathways.[15] Electrospinning has been used to create a variety of new materials, including high strength composites,[16,17] pharmaceutical agents,[17,18] textiles,[19,20] and filtration media,[21,22] but no report has been published on hybrid organic/inorganic membranes with improved protogenic transport with such fiber morphology. In the past, challenges existed to produce electrospun sol-gel based fibers for silica-hybrid PEMFC membranes because the slow hydrolysis and condensation reactions of the silica precursor deemed it too difficult and rather inconsistent. But recently, some nanostructured silica fibers have been achieved.[23–27] However, this system is purely inorganic and no properties were measured. Further, there are few reports on electrospinning PEMFC membranes, but they concern only sulfonated homogeneous polymeric blends.[27–31] In this work, we have optimized our chemistry to our processing, electrospinning, for synthesizing hybrid membranes. The electrospinning of a "sol-gel" solution containing (2-(4-chlorosulfonylphenylethyltrichlorosilane, (CSPTC) with tetraethyl orthosilicate (TEOS), polyvinylidenefluoride-hexafluoropropylene (PVDF-HFP) in dimethylformamide gives rise to the formation of hybrid organic-inorganic membranes. These inorganic-hybrid precursor solutions constitute the base composition. The membranes are processed as described in the Experimental Section to form hybrid membranes with different microstructures.

The tangible properties of these electrospun organic-inorganic membranes are white, uniform and flexible. The membranes, itself, exhibit a micrometer-sized interconnection of

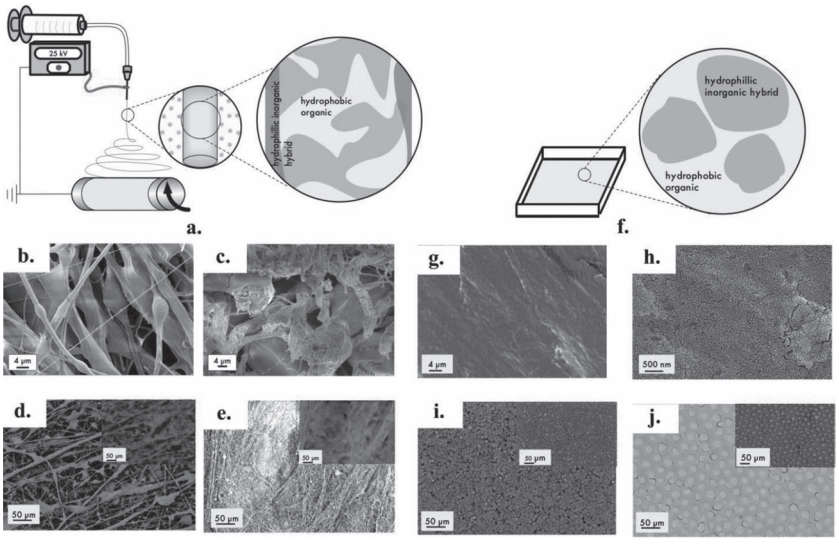

Figure 1. Processing and microstructure. a) The electrospinning process with schematic of the percolated amphiphilic network: inorganic hydrophilic hybrid shell (grey) and hydrophobic organic (yellow). b) Top view of EHM-8, an electrospun hybrid membrane system. c) Cross-section of EHM-8 highlighting the shell around a bundle of fibers. d) Secondary image and X-ray mapping image (inset) of EHM-8. Purple: fluorine, pink: silicon). e) Secondary image and X-ray mapping image (inset) of EHM-4. Purple: fluorine, pink: silicon. f) The casting process with schematic of phase separated amphiphilic components. g.) Top view of CHM-8, a casted hybrid membrane system. h) Magnified region of CHM-8, highlighting the textured surface. i) Secondary image and X-ray mapping image (inset) of CHM-8. Purple: fluorine, pink: silicon). j) Secondary image and X-ray mapping image (inset) of CHM-4. Purple: fluorine, pink: silicon).

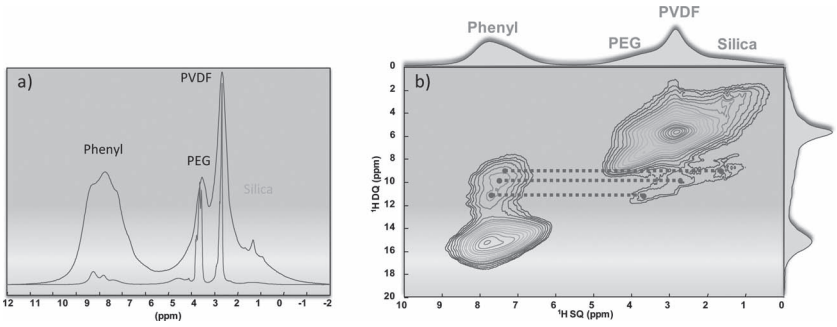

Figure 2. a) ^{1}H MAS NMR spectra of electrospun hybrid membrane (blue) versus casted one (red). b) ^{1}H DQ MAS spectrum of electrospun hybrid membrane that displays the close proximity between the phenyl sulfonated and the PEG, PVDF and silica moities (dotted red lines).

fibers (Figure 1b–e). The electrospun mats investigated through elemental X-ray mapping (Figure 1d,e) show an intimate mixture associated with the PVDF-HFP and the sulfonic acid functionalized silane. On the contrary, the casted membranes are less resilient during handling and have apparent large-scale phase segregation with discreet spherical islands of hydrophilic silica-hybrids embedded in PVDF-HFP, as seen in Figure 1i,j. A casted membrane with only the base components has silica-rich regions (CHM-2) in the range of 15 µm. In contrast, the hybrid membranes containing the hydroxide functionalized fluorinated oligomer present silica-rich regions with average diameters reduced to ≈5 µm, confirming that the additive modified the interfacial region of the segregated regions.

We quantified the hybrid organic-inorganic interfaces in nano-materials using solid-state NMR.[32] ^{1}H MAS (magic angle spinning) NMR spectrum (**Figure 2**a) revealed that for both an identical composition and thermal treatment, the dynamic of the chemical moieties that compose the casted and the electrospun membranes is very different. The relatively broad ^{1}H resonances of the electrospun samples is the signature of protons interacting closely to other components whereas the sharp signals of the casted sample is representative of the high local dynamic of the components in the membrane (polyethylene glycol (PEG) and PVDF in particular). Spatial connectivities can be established by using the ^{1}H–^{1}H dipolar interaction through double quantum (DQ) experiment[33] which establishes contacts between dipole-dipole coupled spins. The Figure 2b displays the ^{1}H DQ MAS spectrum of the electrospun membrane. Cross peaks between the phenyl-sulfonated moiety and the other chemical components of the membranes (PEG, PVDF, silica) are an evidence of the close proximity (<5–6 Å) between these species. These results show that the proton network in the electrospun membranes differs from the casted samples. Additionally, the different chemical components in the electrospun membranes are relatively well entwined (Figure 2b). We believe that this difference in microstructure could explain the variation in the conductivity values (casted vs. electrospun membranes).

As the main properties (proton conductivities, mechanical properties, sorption, etc.) in these membranes does strongly depend on the microstructure of the membrane, we examined the effects of processing (casting versus electrospinning) and the sol-gel chemistry by adding different components in the base-solution including, polyethylene glycol (PEG), dicarboxylated PEG, ethylene hydroxy functionalized fluorinated-oligomer (UPMC-04) and/or 1H,1H,2H,2H perfluorodocytrichlorosilane (PFCTS) on the ion-exchange-capacity (IEC) value and the proton conductivity values (see **Table 1**). These membranes are designed for high temperature-PEMFC, thus, the conductivity values are listed at 120 °C for two different humidity ratios, 50% RH and 80% RH. PEG was used as it improves the physical-properties of the Nafion-based solution for electrospinning process.[27] For EHM8, the proton conductivity was first estimated as function of the thickness of the membrane. We note that the conductivity values are slightly affected with thickness ranging from 10 to 40 µm (see Supporting Information, Table 1). A strong modification of the conductivity values is observed when the thickness of the electrospun membranes exhibits value below 10 µm. This is correlated to a modification of their microstructure. The conductivity values reported in Table 1 exhibit comparable thicknesses (≈15 µm).

For the same composition, the electrospun membranes exhibit higher values for the proton conductivity at 120 °C under 80%RH and experimental IEC values compared to that of the casted ones. For example, EHM-8 exhibits a proton conductivity of 101 mS/cm while the one for CHM-8 is 1.2 mS/cm. This difference is explained by the lowest IEC_{exp} value for the CHM-8 membrane (0.59) and more probably by the dissimilarity between the two microstructures. Indeed, the CHM-8 membrane has silica-island rich regions that are not connected to each other, impeding a 3D continuous pathway for protons throughout the membranes (see Figure 1j,i.). In parallel, we have also measured the proton conduction at 80 °C under various relative humidities. The EHM-8 membranes have proton conductivity comparables to Nafion. A value of 30 mS/cm under 50% of humidity at 80 °C is achieved while the casted hybrid membrane exhibits value close to 1 mS/cm under the same conditions.

Proton transport in these membranes is linked to the nature and the microstructure of the hydrophilic/hydrophobic interfaces.[4] To elucidate the structure-proton transport relationship underlying those organic-inorganic membranes, we performed small-angle neutron scattering (SANS) on both casted and electrospun membranes.[34–37] The SANS data are presented in **Figure 3** for solution-casted membranes and in **Figure 4** for electrospun membranes. Additionally, we performed the contrast variation technique to analyze the complex structure of these multi-component systems.[10,29,35] The membranes were first equilibrated in a mixture of H_2O and D_2O having the same average scattering cross-section as the hydrophobic nuclear vicinity. This approach allows probing into the hydrophilic/hydrophobic interfaces, e.g., mainly inorganic/organic interfaces (Figure 3b and 4b).

The SANS data of the casted hybrid membranes (Figure 3) reveal a hierarchical structure at different length scale. For the casted membrane, we delineate three different zones corresponding to different organic-inorganic interfaces. For high q, the peak at 0.15 $Å^{-1}$ is attributed to silica/water interface. A peak

Table 1. Comprehensive list of values for the calculated and measured compositions, IEC, conductivities, water uptake and dimensional changes for the electrospun hybrid membranes (EHM) and casted hybrid membranes (CHM).

Sample	SiO_2 [%]	PVDF [%]	Additives [%]	Theor. IEC [mEq/g]	Exp. IEC [mEq/g]	σ120 °C/50%R H [mS/cm]	σ120 °C/80%R H [mS/cm]	H_2Ou ptake [%]	Dimensional Changes [%]
EHM-1	11.8	68.8	0	1.99	1.44	**	**	**	**
EHM-2	27.4	48.7	0	1.40	1.09	12.1	60.3	312	26.7
EHM-3	35.09	38.5	0	1.16	1.08	14.1	43.7	170	19.6
EHM-4	19.40	34.9	28.4	1.66	0.62	20.6	82.8	136	19.4
EHM-5	7.37	37.8	42.7	1.23	1.22	3.0	14.1	95	81.3
EHM-6	8.7	35.9	26.4	1.08	0.97	9.6	68.5	138	–7.37
EHM-7	21.1	38.4	31.1	1.15	0.54*	2.5*	20.9*	133*	6.8*
EHM-8	17.2	30.9	44.4	0.93	0.88	15	101	155	16.9
EHM-9	24.1	38.2	28.5	1.15	0.27	**	**	**	**
EHM-10	21.1	31.1	35.5	1.15	1.11	6.32	35.6	76	10
CHM-1	11.8	68.8	0	1.99	**	**	**	**	**
CHM-2	27.4	48.7	0	1.40	0.46	4.24	0.00143	28	52.1
CHM-3	35.09	38.5	0	1.16	0.54	0.0011	2.57	4.5	–10.6
CHM-4	19.40	34.9	28.4	1.66	0.72	0.066	1.76	6.2	–13.5
CHM-5	7.37	37.8	42.7	1.23	0.77	1.3	17.3	0	–9.8
CHM-6	8.7	35.9	26.4	1.08	0.62	1.53	18.0	33	20
CHM-7	21.1	38.4	31.1	1.15	1.093	**	**	21	22
CHM-8	17.2	30.9	44.4	1.15	0.59	0.12	1.2	23	11.11
CHM-9	24.1	38.2	28.5	1.15	**	**	**	**	**
CHM-10	21.1	31.1	35.5	1.15	**	-	**	**	**

*Sample had to be hot pressed to obtain a flat membrane. Any others were used in the green state. ** Membrane unable to be fabricated reproducibly.

at this q corresponds to "ionomer" peak in PEMFC membranes. The intensity of this peak evolves with both the humidity and the D_2O content. At these large scales, the absolute intensities are generally very sensitive to the background subtraction but nonetheless the $q^{-1.8}$ power laws remain far from the q^{-4} ones usually obtained with the ionomer membranes as Nafion[37,38] or sulfonated polyetherketones (KD 97). Though the ionic domains have similar sizes, this result reveals very rough interfaces. The inorganic nature, mainly concerned in this q range, prevents probably the surface restructuration notably of the ionic groups. Additionally, the theoretical neutron scattering length densities (SDL) for PEG is 0.65×10^{10} cm^{-2}. This value combined with the physical-chemical properties of the PEG shows that it is more localized in these hydrophilic zones.

An upturn in intensity is then observed at lower q with a power law close to q^{-2}. This behavior corresponds to locally

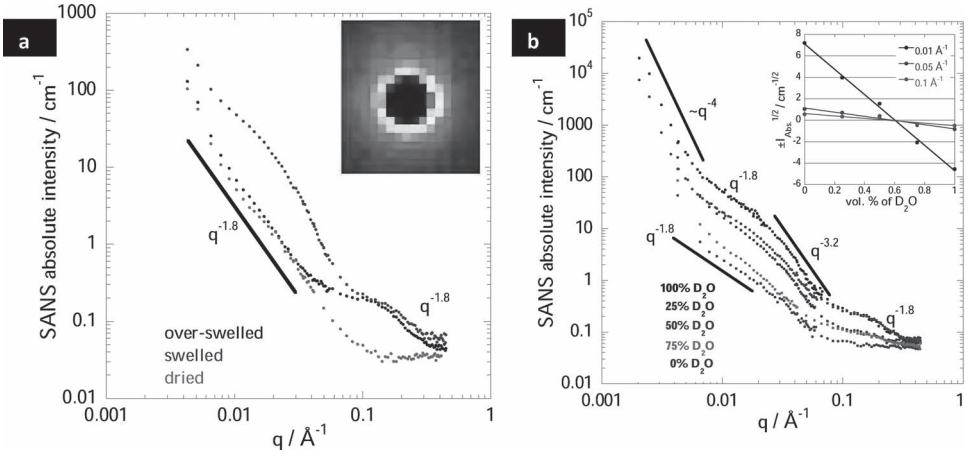

Figure 3. Neutron scattering. a,b) Scattered intensity versus scattering-vector modulus for different swelling states with a low q-range 2D pattern (inset) (a), and for different solution isotopic compositions with index matching graphs (inset) (b) for casting membranes (CHM-8 membranes).

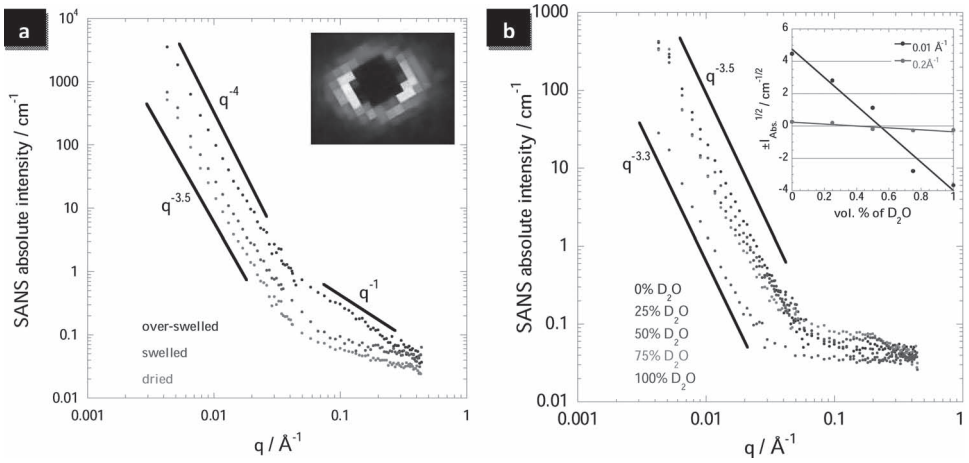

Figure 4. Neutron scattering. a,b) Scattered intensity versus scattering-vector modulus for different swelling states with a low *q*-range 2D pattern (inset) (a) and for different solution isotopic compositions with index matching graphs (inset) (b) for electrospin membrane (EHM-8 membranes).

lamellar microstructure and is attributed to the semi-crystalline structure of the PVDF-HFP matrix; this is consistent with results obtained on hybrid organic-inorganic membranes. This crystalline component is pretty broad and weak suggesting that the introduction of inorganic species in the polymer matrix disrupts the crystalline structure of PVDF-HFP.[6] This is an evidence of a good dispersion of inorganic species.

At intermediate *q* (0.01 and 0.1 Å), we examine the interfaces of hybrid-SiO_2-water objects with the polymer. Those interfaces evolve with the swelling and the D_2O content in the membrane. The SANS intensity curves obey a power law of $q^{-1.8}$ for dried and swelled membranes, which is a signature of elongated, flat objects.[38] For swelled membranes, we do see a change in the intensity and the power law, indicating objects with less-defined shapes with a surface fractal exhibiting dimension of $D_f = 2.8$. The power law is defined as 6-D_f for a 3D object.[39] More interestingly, the scattering signal in this domain (inset Figure 3b) extinguishes for mixtures ranging from 60 to 55% D_2O, which corresponds to neutron SDL of 3.6×10^{10} cm^{-2} and 3.2×10^{10} cm^{-2}, respectively (inset Figure 3b) The theoretical SLD of the PVDF-HFP can be evaluated around 3.2×10^{10} cm^{-2} in the bulk state assuming for the polymer density 1.78 g/cm^{-3}. This observation implies that the polymer is present in every interface with the hydrophilic domains.

In the low *q* region, the presence of well-defined water-polymer interfaces from few hundred to few tens nanometers (power law ~ q^{-4}) is observed. This interface is well-defined in large scale of lengths. The theoretical SDL of functionalized fluorinated-oligomer (2.6×10^{10} cm^{-2}) combined with the physical-chemical properties of these "free-moving" additives indicates that this component is located at this hybrid interface.

Those experiments indicate that a fractal-like structure bridges these different objects from the micrometer to few nanometers. This is correlated to the repetition of the $q^{-1.8}$ behavior at different length scales. These experiments complete the information obtained by SEM, which gives information on objects ranging from the micrometer to the nanometer scale (≈100 nm). The silica domains (micrometer size) observed with SEM are constituted by oblong-like disc with smooth hybrid interfaces.

In contrast to solution-cast membranes spectra which are isotropic (Figure 3a), scattering profile for electrospun membranes present an anisotropy at very low angles (Figure 4a). The SANS spectra (Figure 4) reveal a structuring through two main *q* regions, below and above 0.05 $Å^{-1}$.

In the high *q* range (0.05–0.45 $Å^{-1}$), the large peak at 0.2 $Å^{-1}$ disappears with a mixture near 40% H_2O and 60% D_2O corresponding to a SDL of 2.3×10^{10} cm^{-2}. This correlation length near 3 nm is essentially due to the hydrophilic domains in functionalized silica. This behavior demonstrates nanophase segregation between hydrophilic and hydrophobic domains like in the casted membranes for the same *q* range. Comparing the SLD, these under-systems contain fewer polymers than in the equivalent ones of the casted membranes. In the transitional *q* region (0.045–0.3 $Å^{-1}$), a q^{-1} behavior is observed for the over-swelled membranes (Figure 4a) indicating elongated objects with correlation distances ranging from 2 to 14 nm. The hump due to the PVDF-HFP intercrystallite correlation lengths near 10 nm emerges around 0.06 $Å^{-1}$ (Figure 4a).

In the low *q* range (0.0043–0.5 $Å^{-1}$), a q^{-4} behavior indicates largest structures having smooth well-defined interfaces. These water/polymer interfaces, confirmed by the index matching (SLD = 3.2×10^{10} cm^{-2}), is rough for the swelled and dried states following a $q^{-3.5}$ power law. Thus, the nanometric inorganic objects get organized during the over-swelling clustering to form elongated bigger objects along the polymer fibres. This larger scale structure ranging from 10 to 150 nm bridge with the fibres in the bundles (Figure 1b) which are near 150 nm in diameter. This sub-micrometric structure results in an anisotropic SANS 2D pattern (Figure 4a) unlike the casted-membrane ones in the same *q* range. The $q^{-3.3}$ power law for the spectrum close to the matching index (55% D_2O) indicates a ramification of the polymer at different length scale and region. The electrospun membranes present a surface-fractal-like structure ranging from the micrometer to ten nanometers. The pattern of this network is a polymer fibber cover core-shelled with nanostructured functionalized silica.

These sets of experiments combined with FE-SEM indicate that the electrospun membrane is constituted of elongated

polymeric aggregates surrounded by SiO_2 network supporting pendant chain of ionic groups. Compared to Nafion where packed elongated hydrophilic aggregates are surrounded with ionic groups, randomly oriented in space at the micrometer-scale, in the electrospun membranes, the conducting chain are supported by a percolated-rigid silica network exhibiting higher dielectric constant and large pore size. This microstructure in the hybrid organic-inorganic membrane modifies both the overall electric field and the confinement effect. These features impact directly the proton and water transport. We note that the as-synthesized hybrid membranes exhibit a proton behavior with the humidity comparable to Nafion, confirming the accessibility of the ionic domains to water. The core-shelled structure of the hybrid organic-inorganic fibres allows water to be "weakly" coupled to hydroxyl or unsatured bound of silica network.

Obtaining dense hybrid membranes using the sol-gel-derived approach is important for its use as an electrolyte, rather than a porous membrane. The conductivity value is slightly affected after hot-pressing the EHM-8 membrane, but drops considerably for the casted membrane. The conductivity value is only 1.2 mS/cm. Since the conductivity values were affected by the post-treatment, we believe that the hydrophilic region is re-organized in the casted membrane where the pathways for protons are not well-connected. Furthermore, when the EHM-8 electrospun membrane was impregnated with hydroxide terminated oligomers of polydimethylsiloxane (PDMS) and 3-chlorophenyethyltrichlorosilane (CSPTC) in order to achieve gas-tight membranes through acidic polymerization reaction between silanol-terminated PDMS, CSPTC and subsequent hydrated silanols surface groups (**Figure 5**a), a small change in the conductivity values was measured. This post-treatment increases the IEC value, due to additional sulfonated groups, to 1.72 meq/g, but does not markedly increase the conductivity value (Figure 5b), attesting that the additional–SO_3H groups do not participate in the conduction mechanism. Additionally, the EHM-8 membrane was tested in a fuel cell (see Supporting Information). An OCV of 0.8 V was achieved for 3–4 h. We demonstrated that the Nyquist plot was comparable to the one observed for Nafion, attesting that the measurement was possible. As suggested by,[44] we have evaluated the ohmic losses due to the membrane resistance and of the part of the membrane in the ohmic losses of the fuel cell is ≈10%. This value compared well the ones observed for Nafion, indicating that the hybrid electrospun membranes exhibit sufficient physical properties to run a fuel cell. However, we are currently developing different interfaces to improve the proton transfer between the membrane and the electrode to limit interface ohmic losses.

In general, we do observe that for the same inorganic-hybrid solution precursors, electrospun samples display a significantly higher experimental (IEC) value, attesting to the above-mentioned scheme of percolated networks of functional acidic moieties of the core-shelled structures achieved through the electrospinning process. In contrast, in the casted membranes, a slower forming process creates discrete silica island dispersed in the PVDF-HFP matrix which is highly hydrophobic. Thereby, the accessibility of the –SO_3H groups is limited and the diffusion of hydrated proton throughout the hydrophilic network is low.

Additives in the hybrid membranes modify the proton conduction behavior, demonstrating their impact on the structure, the microstructure of the functionalized inorganic network in the hydrophobic matrix. Hydroxy functionalized fluorinated oligomer and dicarboxylate poly-ethylene glycol (PEG) imparts to membranes an increase in the proton conduction. For example, the membrane EHM-4 containing carboxylic-PEG exhibits proton conductivity of ≈83 mS/cm which is almost two times higher than the one for EHM-3. But, the lack of covalent bonding to the moieties is predicted to cause leaching over time, thus indicating these additives should not be a viable component candidate.

Substituting CSPTC by PFSTC yields membranes with comparable IEC_{exp} values but lower conductivity values. Indeed, EHM-10 exhibits conductivity value of 30 mS/cm while EHM-8 has proton conduction of 101 mS/cm. An explanation is that the reactive fluorinated silanes during the electrospinning process, orientates the fluorinated

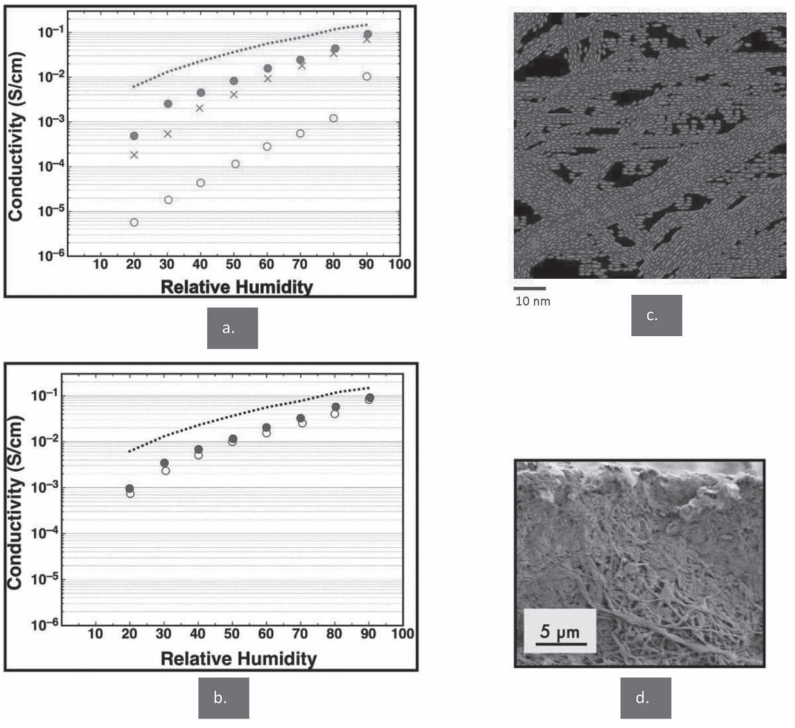

Figure 5. Post-processing comparisons and schematics: a) Comparison of proton conductivity for EHM-8 electrospun membrane (filled circles), hot-pressed EHM-8 electrospun membrane (X), CHM-8 (open circles) and Nafion (dotted line) at 120 °C. b) Comparison of proton conductivity for EHM-8 electrospun membrane (filled circles) and Composite of PDMS-EHM-8 (open circles) electrospun membrane and Nafion (dotted line) at 120 °C. c) Schematic of electrospun hybrid organic-inorganic membranes derived from SANS studies. d) Cross-sectional view of electrospun membrane impregnated with PDMS (PDMS-EHM-8).

chains to the surface and may causes a repulsion of water molecule. This behavior affects the performance of the fuel cell.

The proton conduction was evaluated at 120 °C as function of the number of humidity cycles (going from 0% RH to 100% RH, several times: 10, an example of set of data is reported Table 2, Supporting Information). We do observe no changes in the conductivity values. This result points out that the proton conduction pathways in the electrospun membrane are not affected with the number of cycles. This shows that in this condition the microstructure of the electrospun membrane is stable.

Silica precursor composition affects the microstructure and then the proton conduction behavior. It seems that a higher TEOS concentration to CSPTC yielded still maintained the same IEC_{exp} value, but it lowered the conductivity from (EHM-2) 60 mS/cm to 44 mS/cm, indicating the role of the TEOS in the formation of the silica network and subsequent effective pathways for proton transport. Without TEOS, the core-shell structure could not be created into a viable and reproducible mat through electrospinning and also casting.

Obtaining a 3D network of proton pathway using the electrospinning approach is important for its use in PEMFC, rather than discreet networks of unconnected silica domains within PVDF-HFP polymer. Since we are unable to create efficient pathways for protons by using the casting approach with the same inorganic-hybrid precursor solutions, we believe that when our precursors solutions are subjected to a high-voltage power source between the spinneret (a syringe needle) and drawn to a grounded target (rotational mandrel), a single fiber is continually pulled. This continuous fiber backbone is attributed to the highly entangled nature of PVDF-HFP.[40] Previously, electrospinning reactive sol-gel alkoxides, continuous hollow fibers are formed due to the in situ reactions, e.g., hydrolysis and condensation, of the alkoxides.[41–43] During the expedient process, this specific microenvironment along the fiber axis continuously exposes the reactive precursors to a high charge accumulation on the surface and atmospheric moisture.[42] Although these precursors are prepared as homogenous solutions, they undergo a rapid and unique phase segregate to form the ultra-structured sulfonic-acid/ silica structures. This unique phase segregation is exclusively due to the reactive chemical coupled electrospinning processing because: 1) sol-gel hybrids continually undergo in situ inorganic polymerization within the very hydrophobic PVDF-HFP fiber construct and 2) reactive sol-gel and sulfonic acid components migrate to the surface of the fiber due to both the polarization and reactivity with atmospheric water to form the core shell nature. The mats have a consistent overall morphology that is varicose and polydispersed in nature (Figure 1b). This is caused by the persistent electrostatic charges trying to overcome the resistant elastic stresses opposed by PVDF-HFP and reactive silica inorganic polymerization. The core-shell formation seems to also engulf the multiple fibers (Figure 1c); we propose the sol-gel species are continually reaction, even as it hits the target.

The mechanical properties are essential for using these membranes in fuel cell. The modulus of both the casting and the electrospun membranes were measured as function of the temperature and compared to Nafion. The casting membranes exhibit moduli more than one order of magnitude lower (6 MPa, 60 °C) than the ones of the electrospun membranes (113 MPa, 60 °C) for all studied temperatures (see Supporting Information, Table 3). In contrast, the modulus of the electrospun membranes is comparable to the one for Nafion up to 60 °C. Above 80 °C, the modulus for Nafion dramatically decreases (3 MPa, 120 °C) while the one for electrospun membrane remains high up to 130 °C (75 MPa, 120 °C). This different behavior might be related to the difference in crystallinity for both casting and electrospun membranes, as evidenced by SANS study. The core-shell structure present in the hybrid membrane gives rise to exceptional mechanical properties at high temperature, attesting its interesting properties for PEMFC application. Additionally, tensile strength and elongation at break have been measured and the values are comparable to Nafion (20 MPa and an elongation at break of 150%). Note that the mechanical properties of these electrospun membranes were modified when impregnation with PDMS was performed. The PDMS-modified electrospun membranes become more fragile and can break easily.

Our sol-gel protocol combined with the electrospinning approach can be readily adapted to prepare other conductive materials polymer-based membranes or additional hybrid organic-inorganic membranes with different conductive groups ($-PO_3H_2$ or $-SO_3H/-PO_3H_2$) and inorganic moieties like TiO_2, ZrO_2 or mixed oxides. Phosphonated groups are interesting for conduction at high temperature and low humidity while TiO_2 or ZrO_2 components would be more stable under the very restrictive fuel cell conditions, e.g. acidic media under low humidity and high temperature. By adding other metal salts during the synthesis of the precursor solutions, homogeneous hybrid precursor solutions are produced containing PVDF, TiO_2, and $SiO_2–SO_3H$. By analogy, we expect that similar composite structures composed of functionalized inorganic moieties and thermostable polymer will contain optimized 3D pathway for proton hopping for use as high-temperature PEMFC membranes.

3. Conclusions

Finally, we can synthesize hybrid organic-inorganic membranes by a judicious combination of hybrid organic-inorganic solutions precursors and the electrospinning process; dense membranes containing–SO_3H groups and thermostable polymer yield conductivity values of 15 mS/cm at 120 °C under 50% RH. By contrast, poor conductivities values (e.g., 1 mS/cm under the same conditions) were achieved using the same hybrid organic-inorganic solutions precursors in combination with the casted process. These different microstructures conduce to membranes with different mechanical behavior. Exceptional high modulus for the electrospun membranes were achieved above 80 °C. Present efforts are devoted to prepare these materials as thick-membranes and evaluating their potential for PEMFC membranes working at higher temperature and low humidity.

4. Experimental Section

Materials Synthesis: PVDF-HFP was dissolved in DMF at 75 °C and cooled to room temperature. For each sample, this PVDF-HFP/ DMF solution was added and mixed into ten hybrid membrane (HM) precursor series.

All solutions were prepared at room temperature and stirred at 70 °C for 3 h in a closed glass vial. They were spun after solutions were allowed to cool to room temperature. All TEOS: CSPTC rations are 2:1 mol, except HM-4 series and HM-5 series. E designed electrospun membrane and C casting membrane. PEG-c denotes carboxylic PEG.

E or CHM-1 PVDF + CSPTC
E or CHM-2 PVDF + CSPTC + TEOS (2TEOS: 1 CSPTC mol)
E or CHM-3 PVDF + CSPTC + TEOS (1TEOS: 1CSPTC mol)
E or CHM-4 PVDF+ CSPTC + TEOS + PEG-c
E or CHM-5 PVDF + CSPTC + PEG + UPMC-04
E or CHM-6 PVDF + CSPTC + TEOS + PEG
E or CHM-7 PVDF + CSPTC + TEOS + UPMC-04
E or CHM-8 PVDF + CSPTC + TEOS + PEG + UPMC-04
E or CHM-9 PVDF + CSPTC + TEOS + PFSCT
E or CHM-10 PVDF + CSPTC + TEOS + PFSCT

Measurements: Analysis of the casted and electrospun membranes.

Characterization of the Membranes: The morphology and the thickness of the membranes were observed by scanning electron microscopy (SEM) (Zeiss, Supra 55) and the elemental mappings were done by using FE-SEM Field emission scanning electron microscope equipped with an energy dispersive X-ray (EDX) detector.

Ion exchange capacity (IEC) is defined as the ration between the number of H^+ (in mmol) and the weight of the dry membrane (mmol H^+/g of the membrane). The membranes were soaked in 1 M NaCl solution for 24 h. The protons released by the exchange reaction with Na^+ ions were titrated against 0.01 M NaOH solution by using phenolphthalein as an indicator. The IEC value was calculated Equation (1) where v is the volume of the NaOH used.

$$\text{Experimental IEC (mmol H}^+\text{/g)} = \frac{v \times [\text{NaOH}]}{\text{weight (hybrid organic} - \text{inorganic membranes)}} \quad (1)$$

Water-Uptake Determination: The water uptake of the membranes was calculated from Equation (2), W_1 is the weight of the wet membrane after immersing in water at RT overnight and W_2 is the weight of the dry membrane.

$$W\,(\text{wt\%}) = ((W_1 - W_2)/W_2) \times 100\% \quad (2)$$

Proton Conductivity: The proton conductivities of the membranes were measured by using a BT-512 In-Plane Membrane Conductivity Test System (BekkTech LLC) under N_2 atmosphere. The in-plane-4-electrode measurement (scanning DC with voltage sweeps from 0.1 V to –0.1 V) was performed at 120 °C for two relative humidities values: 50% and 80% RH). The dry dimensions of the membrane are considered for calculations. The thickness is about 15 µm.

Small-Angle Neutron Scattering: SANS experiments were carried out with the PAXE spectrometer in the Leon Brillouin Laboratory (Saclay, France). Two sample-to-detector distances (SDD) and neutron wavelengths (λ) were used to cover magnitudes of the scattering vector modulus q from 0.004 to 0.44 $Å^{-1}$ (λ = 12 Å, SDD = 4 m, and λ = 5 Å, SDD = 1.5 m). The resulting flat level of the scattering intensity at the high q values is of the order of magnitude of the experimental background.

Dynamical Mechanical Analysis: DMA was performed on a Vicoanalyseur VA2000 (Metravib R.D.S.) as a function of temperature and a constant water pressure of pH_2O = 24 hPa (mbar). The maximum elongation was 20 µm at the frequency of 3 Hz (sample dimensions typically in the range of 5 mm × 2 mm × 0.15–0.35 mm).

Supporting Information

Supporting Information is available from the Wiley Online Library or from the author.

Acknowledgements

This work was supported by the LRC program through the CEA Ripault. J.B. acknowledges a postdoctoral research fellowship (2007-2008). V.M. acknowledges the NSF program a post-doctoral research fellowship (2009-2010). The authors thank J. Jestin as a local contact on the PAXE spectrometer.

Received: September 17, 2012
Published online: January 17, 2013

[1] C. Laberty-Robert, K. Vallé, F. Pereira, C. Sanchez, *Chem. Soc. Rev.* **2011**, *40*, 961.
[2] D. D. Jones, J. Rozière, *Adv. Polym. Sci.* **2008**, *215*, 219.
[3] O. Sel, C. Laberty-Robert, T. Azais, C. Sanchez, *Phys. Chem. Chem. Phys.* **2009**, *11*, 3733.
[4] O. Sel, A. Soules, B. Ameduri, B. Boutevin, C. Laberty-Robert, G. Gebel, C. Sanchez, *Adv. Funct. Mater.* **2010**, *20*, 1090.
[5] O. Sel, T. Azais, M. Marechal, G. Gebel, C. Laberty-Robert, C. Sanchez, *Chem. Asian J.* **2011**, *6*, 11, 2992.
[6] F. Niepceron, B. Lafitte, H. Galiano, J. Bigarre, E. Nicol, J. F. Tassin, *J. Membr. Sci.* **2009**, *338*, 100.
[7] K. Schmidt-Rohr, Q. Chen, *Nat. Mater.* **2008**, *7*, 75.
[8] K. A. Mauritz, R. B. Moore, *Chem. Rev.* **2004**, *104*, 4535.
[9] T. Ohkubo, K. Kidina, A. Ohira, *Macromolecules* **2008**, *41*, 8688.
[10] L. Rubatat, A. L. Rollet, G. Gebel, O. Diat, *Macromolecules* **2002**, *35*, 4050.
[11] T. D. Gierke, G. E. Munn, F. C. Wilson, *J. Polym. Sci.* **1981**, *19*, 1687.
[12] P. C. van der Heijden, L. Rubatat, O. Diat, *Macromolecules* **2004**, *37*, 5327.
[13] O. Sel, L. To Thi Kim, C. Debiemme-Chouvy, C. Gabrielli, C. Laberty-Robert, H. Perrot, C. Sanchez, *Electrochem. Commun.* **2010**, *12*, 8, 1136.
[14] K. Valle, P. Belleville, F. Pereira, C. Laberty-Robert, C. Sanchez, J. D. Bass, FR2958184; WO/2011/124622, **2011.**
[15] O. Diat, G. Gebel, *Nat. Mater.* **2008**, *7*, 13.
[16] K. C. Krogman, J. L. Lowery, N. S. Zacharia, G. C. Rutledge, P. T. Hammond, *Nat. Mater.* **2009**, *8*, 512.
[17] S. M. Liff, N. Kumar, G. H. McKinley, *Nat. Mater.* **2007**, *6*, 76.
[18] M. F. Pittenger, A. M. Mackay, S. C. Beck, R. K. Jaiswal, R. Douglas, J. D. Mosca, D. W. Simonetti, S. Craig, D. R. Marshak, *Science* **1999**, *284*, 143.
[19] P. W. Y. Dankers, M. C. Harmsen, L. A. Brouwer, M. J. A. Van Luyn, E. W. Meijer, *Nat. Mater.* **2005**, *4*, 568.
[20] M. P. Prabhakaran, L. Ghasemi-Mobarakeh, S. Ramakrishna, *J. Nanosci. Nanotechnol.* **2011**, *11*, 3659.
[21] W. Sambaer, M. Zaltoukal, D. Kimmer, *Chem. Eng. Sci.* **2011**, *66*, 613.
[22] A. M. Bazargan, M. Keyanpour-rad, F. A. Hesari, M. E. Ganji, G. M. Esmaeilpour, *Desalination* **2011**, *265*, 148.
[23] Z. J. Ma, H. J. Ji, Y. Teng, G. P. Dong, J. J. Zhou, D. Z. Tan, J. R. Qiu, *J. Colloid Interface Sci.* **2011**, *358*, 547.
[24] A. Greiner, J. H. Wendorff, *Angew. Chem. Int. Ed.* **2007**, *46*, 5670.
[25] Y. J. Kim, C. H. Ahn, M. B. Lee, M. S. Choi, *Mater. Chem. Phys.* **2011**, *127*, 137.
[26] S. Wen, L. Liu, L. Zhang, Q. Chen, L. Zhang, H. Fong, *Mater. Lett.* **2010**, *64*, 1517.
[27] J. B. Ballengee, P. N. Pintauro, *J. Electrochem. Soc.* **2011**, *158*, B568.
[28] J. B. Ballengee, P. N. Pintauro, *Macromolecules* **2011**, *44*, 7307.
[29] B. Dong, L. Gwee, D. Salas-de la Cruz, K. I. Winey, Y. A. Elabd, *Nano Lett.* **2010**, *10*, 3785.
[30] J. Choi, K. M. Lee, R. Wycisk, P. N. Pintauro, P. T. Mather, *Macromolecules* **2008**, *41*, 4569.

[31] S. Madhugiri, A. Dalton, J. Gutierrez, J. P. Ferraris, K. J. Balkus, *J. Am. Chem. Soc.* **2003**, *125*, 14531.
[32] C. Bonhomme, C. Coelho, N. Baccile, C. Gervais, T. Azaïs, F. Babonneau, *Acc. Chem. Res.* **2007**, *40*, 738.
[33] M. Feike, D. E. Demco, R. Graf, J. Gottwald, S. Hafner, H. W. Spiess, *J. Magn. Reson., Ser. A* **1996**, *122*, 214.
[34] *Neutron, X-rays and light scattering: Introduction to an investigate tool for colloidal and polymeric systems*, (Eds: P. Lindner, T. Zemb), North-Holland Elsevier, Amsterdam **1991**.
[35] C. Cailleteau, F. Angeli, F. Devreux, S. Gin, J. Jestin, P. Jollivet, O. Spalla, *Nat. Mater.* **2008**, *7*, 978.
[36] K. D. Kreuer, *J. Membr. Sci.* **2001**, *185*, 29.
[37] G. Gebel, J. Lambard, *Macromolecules* **1997**, *30*, 7914.
[38] *Small Angle X-ray Scattering*, (Eds: O. Glatter, O. Kratky), Academic Press, London **1982**.
[39] H. D. Bale, P. W. Schmidt, *Phys. Rev. Lett.* **1984**, *53*, 596.
[40] T. T. Nguyen, J. S. Park, *J. Appl. Polym. Sci.* **2011**, *121*, 3596.
[41] S. Madhugiri, B. Sun, P. G. Sminiotis, J. P. Ferraris, J. R. Balkus, *Microporous Mesoporous Mater.* **2004**, *69*, 77.
[42] Y. L. Cheah, N. Gupta, S. S. Pramana, V. Aravindan, G. Wee, M. Srinivasan, *J. Power Sources* **2011**, *196*, 6465.
[43] J. Leng, S. Li, Z. Wang, Y. Xue, D. Xu, *Mater. Lett.* **2010**, *64*, 1912.
[44] M. Ciureanu, R. Roberge, *J. Phys. Chem. B* **2001**, *105*, 3531.